2009 American Control Conference
Hyatt Regency Riverfront, St. Louis, MO, USA
June 10-12, 2009

Robust Control of a Piezoelectric Stage under Thermal and External Load Disturbances

Mohammad Motamedi, Seyed Mehdi Rezaei, Mohammad Zareinejad, and Mozafar Saadat

Abstract— **Piezoelectric actuators are widely used in micromanipulation tasks such as Atomic Force Microscopy and Cell Manipulation. However, the hysteresis nonlinearity and the creep reduce their fidelity and cause difficulties in the micromanipulation control procedure. Besides, variation of temperature and external loads could change the model parameters identified for the piezo actuator. In this paper, a novel feedforward-feedback controller is proposed. The Prandtl-Ishlinskii model is utilized to linearize the actuator hysteresis in feedforward scheme and a sliding mode based impedance control with perturbation estimation is used to cancel out the thermal and external load disturbances in feedback scheme. The efficiency of the proposed controller is verified by experiments.**

I. Introduction

Piezoceramics hold great promise as smart sensors and actuators in a variety of applications. Micromanipulation, aerospace and bio-medical systems for improving performance and to augment stability are such examples. It is well known that the piezoelectric actuator has many advantages such as: (1) there are no moving parts; (2) the actuators can produce large forces; (3) they have almost unlimited resolution; (4) the efficiency is high; (5) response is fast. The major limitation of piezoceramic actuators is their nonlinear hysteretic behavior that leads to performance degradation in precision positioning applications [1]. The maximum error due to hysteresis is found to be as much as 10-15% of the path covered if the actuators are run in an open-loop fashion. This error affects the system performance.

To deal with the effect of hysteresis, feedforward and feedback techniques have been proposed. In the open-loop technique (feedforward), a model with high precision is needed in order to model the hysteresis. The key idea of a feedforward controller is to cascade the inverse of the hysteresis model with the actual hysteretic plant. In this manner, an identity mapping between the desired output and actuator response can be provided.

Preisach [2]-[5], and Prandtl-Ishlinskii (PI) [6] are the well-known feedforward models. Implementation complexity is the major setback of Preisach model. PI is less complex and its inverse can be computed analytically. Identification of PI model is performed for a single loop. Therefore, in feedforward scheme, any deviation from the identified loop leads to hysteresis compensation error.

In this study a modified PI model [7] is applied and its inverse is used to cancel out the hysteresis effect. The nonlinear piezoelectric actuator is linearized using feedforward inverse hysteresis. The linearized uncertain model is used to design the controller [8].

To deal with the influence of parametric uncertainties, external disturbance effects and PI identification error, a perturbation term is considered in linearized model. For proper trajectory tracking, a sliding mode based impedance control with perturbation estimation is proposed.

In order to evaluate the proposed approach, performance of the piezoelectric actuator in trajectory tracking under thermal and load disturbances is investigated.

II. Piezo Stage and Hysteresis Modeling

A. Dynamic Modeling for the Piezo Stage

The piezo stage consists of a 1-DOF stage actuated by a piezo stack actuator. In many investigations, a second-order linear dynamics has been utilized for describing the system dynamics. As shown in Fig. 1, this model combines mass-spring-damper ratio with a nonlinear hysteresis function appearing in the input excitation to the system.

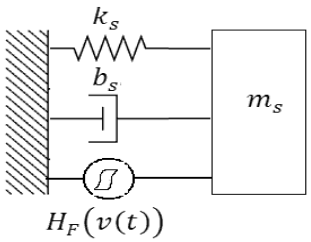

Fig. 1. Piezoelectric actuator

The following equation defines the model:

$$m_s\ddot{x}_s(t) + b_s\dot{x}_s(t) + k_s x_s(t) = H_F(v(t)) \qquad (1)$$

where $x_s(t)$ is the stage position. m_s, b_s and k_s are stage mass, viscous coefficient and stiffness, respectively. $H_F(v(t))$ denotes the hysteretic relation between input voltage and excitation force. Piezoelectric actuators have very high stiffness, and consequently possess very high natural frequencies. In low-frequency operations, the effects of actuator damping and inertia could be safely

Manuscript received September 22, 2008.

Mohammad Motamedi is with the Department of Mechanical Engineering, Amirkabir University of Technology, Tehran, Iran (corresponding author to provide phone: +989123331016; e-mail: mohammad.motamedi@gmail.com).

neglected. Hence, the governing equation of motion is reduced to the following static hysteresis relation between the input voltage and actuator displacement:

$$x(t) = \frac{1}{k_s} H_F\big(v(t)\big) = H_x\big(v(t)\big)$$
$$\{m_s \ddot{x}_s(t) \ll b_s \dot{x}_s(t) \ll k_s x_s(t)\} \quad (2)$$

Equation (2) facilitates the identification of the hysteresis function $H_F\big(v(t)\big)$ between the input voltage and the excitation force. This is performed by first identifying the hysteresis map between the input voltage and the actuator displacement, $H_x\big(v(t)\big)$. It is then, scaled up to k_s to obtain $H_F\big(v(t)\big)$.

$$m_s \ddot{x}_s(t) + b_s \dot{x}_s(t) + k_s x_s(t) = k_s H_x\big(v(t)\big) \quad (3)$$

To consider the influence of parametric uncertainties, unmodeled dynamics, and identification error, a perturbation term $P(t)$ is added to the stage model. Thus the stage model (1), can be rewritten in the following form:

$$m_s \ddot{x}_s(t) + b_s \dot{x}_s(t) + k_s x_s(t)$$
$$= H_F\big(v(t)\big) + P(t) = k_s H_x\big(v(t)\big) + P(t) \quad (4)$$

To consider the interaction with environment, the force F_e exerted by the environment is inserted into the model. Therefore, the dynamic model of piezo stage can be written as follows:

$$m_s \ddot{x}_s(t) + b_s \dot{x}_s(t) + k_s x_s(t)$$
$$= k_s H_x\big(v(t)\big) + P(t) - F_e \quad (5)$$

B. Hysteresis Modeling

In this section the hysteresis modeling using Prandtl-Ishlinskii (PI) is described. This model can approximate the hysteresis loop accurately and its inverse could be obtained analytically. Therefore, it facilitates the inverse feedforward control design.

1) Prandtl-Ishlinskii (PI)

There is a backlash operator in the PI hysteresis model that is defined by:

$$y(t) = H_r[x, y_0](t)$$
$$= max\{x(t) - r, min\{x(t) + r, y(t - T)\}\} \quad (6)$$

where x is the control input, y is the actuator response, r is the control input threshold value or the magnitude of the backlash and T is the sampling period. The initial consistency condition of (6) is given by:

$$y(0) = max\{x(0) - r, min\{x(0) + r, y_0\}\} \quad (7)$$

where y_0 is usually but not necessarily initialized to zero. Multiplying the backlash operator H_r by a weight value w_h, the generalized backlash operator is obtained:

$$y(t) = w_h H_r[x, y_0](t) \quad (8)$$

The weight w_h defines the gain of the backlash operator and may be viewed as the gear ratio in gear mechanical play analogy. Complex hysteresis nonlinearity can be modeled by a linear weighted superposition of many backlash operators with different threshold and weight values:

$$y(t) = \boldsymbol{w_h^T H_r}[x, \boldsymbol{y_0}](t) \quad (9)$$

where

$$\boldsymbol{H_r}[x, \boldsymbol{y_0}](t) = [H_{r0}[x, y_{00}](t) \dots H_m[x, y_{0n}](t)]^T \quad (10)$$

With the weight vector $\boldsymbol{w_h^T} = [w_{h0} \dots w_{hn}]$, the threshold vector $\boldsymbol{r} = [r_0 \dots r_n]^T$ where $0 = r_0 < \cdots < r_n$ and the initial state vector $\boldsymbol{y_0} = [y_{00} \dots y_{0n}]^T$. The control input threshold values r_n are usually chosen to be of equal intervals between maximum and minimum of piezoelectric actuator displacement.

2) Modified PI Operator

The PI operator inherited the symmetry property of the backlash operator about the center point of the loop formed by the operator. The fact that most real actuator hysteretic loops are not synonymic weakens the model accuracy of the PI operator. To overcome this restrictive property, a saturation operator is combined in series with the hysteresis operator. A saturation operator is a weighted superposition of linear-stop or one-sided dead zone operators. A dead zone operator is a non-convex, non-symmetrical and memory free nonlinear operator given by:

$$S_d[x](t) = \begin{cases} max\{x(t) - d, 0\} & d > 0 \\ x(t) & d = 0 \end{cases} \quad (11)$$
$$z(t) = \boldsymbol{w_s^T}.\boldsymbol{S_d}[y](t)$$

where y is the output of the hysteresis operator and z is the actuator response. $\boldsymbol{w_s^T} = [w_{s0} \dots w_{sn}]$ is the weight vector. $\boldsymbol{S_d}[y](t) = [S_{d0}[y](t) \dots S_{dm}[y](t)]$, with the threshold vector $\boldsymbol{d^T} = [d_0 \dots d_n]^T$, $0 = d_0 < \cdots < d_m$.
Thus the modified PI operator is defined as follows:

$$y(t) = \boldsymbol{w_s^T}.\boldsymbol{S_d}\left[\boldsymbol{w_h^T}.\boldsymbol{H_r}[x, \boldsymbol{y_0}]\right](t) \quad (12)$$

d_i is usually chosen to be equal intervals between maximum and minimum of hysteresis operator output.

3) Inverse model of PI

The inverse PI operator is given by

$$H^{-1}(t) = \boldsymbol{w_h^T H_{r'}}[\boldsymbol{w_s^T}.\boldsymbol{S_d}[z], \boldsymbol{y_0'}](t) \quad (13)$$

Cascading the inverse hysteresis model with the actual hysteresis model gives the identity mapping between the control input $x_d(t)$ and the actuator response $x(t)$.

$$x(t) = H^{-1}[H[x_d(t)]] \quad (14)$$

The inverse model parameters can be calculated analytically

as follow:

$$w'_{h_0} = {}^{1}/_{w_{h_0}} ; w'_{s_0} = {}^{1}/_{w_{s_0}} \quad (15)$$

$$w'_{h_i} = \frac{-w_{h_i}}{\left(\sum_{j=0}^{i} w_{h_j}\right)\left(\sum_{j=0}^{i-1} w_{h_j}\right)} , i = 1 \dots n; \quad (16)$$

$$w'_{s_i} = \frac{-w_{s_i}}{\left(\sum_{j=0}^{i} w_{s_j}\right)\left(\sum_{j=0}^{i-1} w_{s_j}\right)} , i = 1 \dots n; \quad (17)$$

$$r'_i = \sum_{j=0}^{i} w_{h_j}\left(r_i - r_j\right), i = 0 \dots n; \quad (18)$$

$$d'_i = \sum_{j=0}^{i} w_{s_j}\left(d_i - d_j\right), i = 0 \dots m; \quad (19)$$

$$y'_{0_i} = \sum_{j=0}^{i} w_{h_j} y_{0_i} + \sum_{j=i+1}^{n} w_{h_j} y_{0_j} , i = 0 \dots n \quad (20)$$

After setting the threshold parameters r and d as described in the previous section, the weight parameters $\boldsymbol{w_h}$ and $\boldsymbol{w_s}$ are estimated by performing a least squares fitting of (12). Graphically, the inverse is the reflection of the resultant hysteresis loop about the 45° line.

4) Feedforward Hysteresis Compensation

The structure of inverse feedforward hysteresis compensation is shown in Fig. 2. The key idea of an inverse feedforward controller is to cascade the inverse hysteresis operator H_x^{-1} with the actual hysteresis represented by the hysteresis operator H_x. In this manner, an identity mapping between the desired actuator output $x_d(t)$ and actuator response $x(t)$ is obtained.

The inverse PI operator H_x^{-1} uses $x_d(t)$ as input and transforms it into a control input $v_{H_x^{-1}}(t)$ which produces $x(t)$ in the hysteretic system that closely tracks $x_d(t)$.

5) Identification of the Hysteresis Model

In this section the method for identification of hysteresis function between the input voltage and the actuator displacement as defined by (12) is described. Weighting parameters are identified using least-squares optimization technique for error minimization. Static hysteresis is identified using quasi-static triangular input. Appropriate values for order of backlash operator n, saturation function m and threshold vectors, $\boldsymbol{r}$ and $\boldsymbol{d}$, are selected for the proper approximation of hysteresis. The values for n and m can be set as 25 and 15, respectively.

Identification of PI parameters is performed for the measured actuator response subjected to 100V p-p sawtooth control input with frequency of $0.5Hz$.

III. Temperature Effect Analysis

In the temperature effect analysis, two effects must be considered:

A. *Linear Thermal Expansion:* Thermal stability of piezoceramics is better than that of most other materials. Actuators and positioning systems consist of a combination of piezoceramics and other materials and their overall behavior differs accordingly.

B. *Temperature Dependency of the Piezo Effect:* Piezo translators work in a wide temperature range. The piezo effect in PZT ceramics is known to function down to almost zero Kelvin. But the magnitude of the piezo coefficients is temperature dependent. It is also noted that closed-loop piezo positioning systems are less sensitive to temperature changes than open-loop systems. Optimum accuracy is achieved if the operating temperature is identical to the calibration temperature. At liquid helium temperature, piezo gain drops to approximately 10–20 % of its room temperature value which causes a displacement error more than $10\mu m$ in the micromanipulation system.

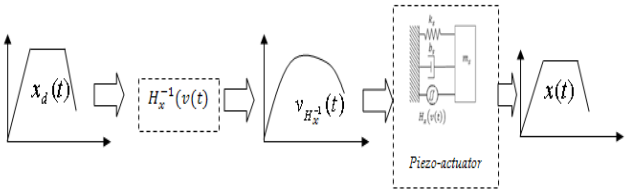

Fig. 2. The feedforward inverse control.

It is well known that as the temperature increases, the creep is amplified. For the representation of this phenomenon in the piezoelectric actuator, a step voltage is applied and the displacement is monitored for about four minutes. As shown in Fig. 3, the creep is considerably amplified .This behavior decreases the accuracy of the micro-positioning system.

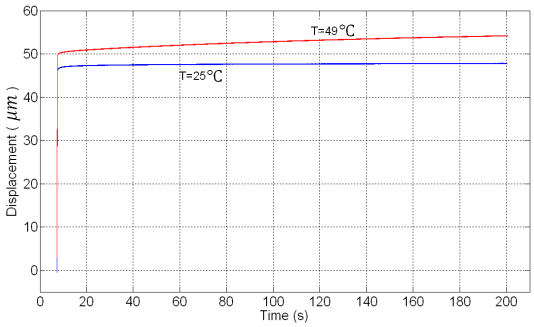

Fig. 3. The effect of thermal disturbance on creep.

The temperature variation, affects the hysteresis as well. To observe that, a sine voltage of 60V of amplitude is applied to the piezoelectric actuator. The resultant hyteretic loops are plotted for two temperatures ($T = 26°C$ and $T = 55°C$). Fig.4 depicts that temperature variations affects the hysteretic behavior.

IV. Impedance Control for the Piezoelectric Actuator with Sliding Mode Based Perturbation Estimation

The desired dynamic for the piezo stage is considered as follows:

$$\bar{m}_s\ddot{\tilde{x}}(t) + \bar{b}_s\dot{\tilde{x}}(t) + \bar{k}_s\tilde{x}(t) = -F_e \quad (21)$$

where $\bar{m}_s$,$\bar{b}_s$ and $\bar{k}_s$ are the desired mass, viscous damping coefficient, and stiffness of piezo-actuator, respectively. $\tilde{x}(t) = x_s - x_d$ is position error and x_d is desired trajectory.

The control law for the piezo stage is obtained by combining (21) and (1):

$$u_s(t) = H_F^{-1}\left\{-\frac{m_s}{\bar{m}_s}\left[b_s\dot{\tilde{x}}(t) + k_s\tilde{x}(t) + F_e(t)\right] + F_e(t) - b_s\dot{x}_s(t) + m_s\ddot{x}_d - P_{est}\right\}. \quad (22)$$

To deal with the influence of parametric uncertainties, unmodeled dynamics and PI identification error, estimation of perturbation term P_{est} is added to the piezo stage model. In next section the procedure for estimation of P_{est} is represented.

A. Perturbation Estimation

[9] and [10] have proposed a perturbation estimation scheme which is embedded in the traditional Sliding Mode Control (SMC) design. The main advantage of this methodology is that a priori knowledge of the upper-bounds of perturbation is not required. The general class of nonlinear dynamics is considered as:

$$x^{(n)} = f(x) + \Delta f(x) + [B(x) + \Delta B(x)]u + d(t) \quad (23)$$

where $X_i = [x_i, \dot{x}_i, \dots, x_i^{(n-1)}]^T \varepsilon R^n, i = 1,2,\dots,m$ is the state subvector and $x_i, i = 1,2,\dots,m$ are m independent coordinates. $\Delta f(x)$ is perturbation of f, $\Delta B(x)$ is perturbation of control gain u and $d(t)$ is system disturbance vector. Perturbations and disturbance are gathered into a variable named perturbation vector:

$$\psi(X,t)_{actual} = \Delta f(x) + \Delta B(t)u + d(t) = x^{(n)} - f - Bu. \quad (24)$$

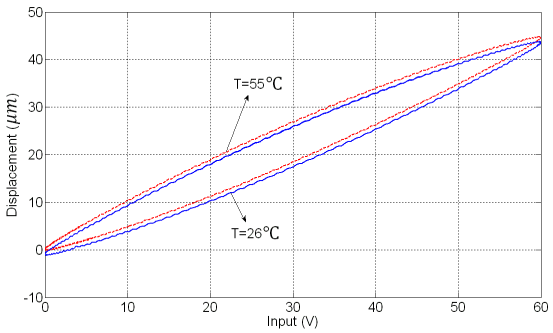

Fig. 4. The effect of thermal disturbance on hysteresis.

If all the components in the dynamics show slower variations with respect to the loop closure (or sampling) speed, $\psi(X,t)$ can be estimated as:

$$\psi(X,t)_{estimated} = x^{(n)}_{calculated} - f - Bu(t-\delta). \quad (25)$$

where δ is the control interval or sampling time in the digital controller. In practice, sampling time is selected high enough to ensure $u(t) = u(t-\delta)$. As shown in (25), the class of perturbation estimator is based on the simple intuition that if all the states are available, the perturbation of the plant can be effectively estimated using the nominal model and one step delayed input signals. Additionally, in the absence of measurements of $x^{(n)}$, an approximation is utilized as:

$$x^{(n)} = \frac{x^{(n-1)}(t) - x^{(n-1)}(t-\delta)}{\delta}. \quad (26)$$

The errors in this estimation appear from two sources:

1) $x^{(n-1)}(t)$ measurements are often noisy. Therefore, their calculated time derivatives may manifest prohibitively large variations. The measurement noise of $x^{(n-1)}(t)$ should be filtered to a suitable level.

2) Regardless of the sampling speed, the inequality $u(t) \neq u(t-\delta)$. holds.

It is important to note that our objective is not to reduce the estimation error to zero. No matter how large the actual perturbations are, smaller perturbation error leads to better performance.

B. Sliding mode based impedance control for piezo stage using perturbation estimation

A modified version of system (1) could be written as:

$$m_s\ddot{x}_s(t) + b_s\dot{x}_s(t) + k_s x_s(t) = H_F\big(v(t)\big) + P_{est}(t) - \tilde{P}(t). \quad (27)$$

where $\tilde{P}(t) = P_{est}(t) - P(t)$ is the error signal between the system perturbations and its estimation.
Based on the perturbation estimation technique, an estimation of the perturbation function given in (27) is obtained as:

$$P_{est}(t) = m_s\ddot{x}_s(t) + b_s\dot{x}_s(t) + k_s x_s(t) - H_F\big(v(t-\delta)\big) \quad (28)$$

Substituting $H_F(v(t))$ by $k_s H_F(v(t))$, using (4) one can obtain:

$$P_{est}(t) = m_s\ddot{x}_s(t) + b_s\dot{x}_s(t) + k_s x_s(t) - k_s H_X\big(v(t-\delta)\big) \quad (29)$$

Sliding surface can be defined as the following:

$$s(t) := \frac{1}{\bar{m}_s}\int_0^t I_e(t)dt \quad (30)$$

where I_e is the impedance error, that is:

$$I_e := \bar{m}_s\ddot{\tilde{x}}(t) + b_s\dot{\tilde{x}}(t) + \bar{k}_s\tilde{x}(t) - (-F_e(t)) \quad (31)$$

Theorem:
For the system described by (6), if the control law is given by:

$$v(t) = u_s(t) = H_F^{-1}\left\{-\frac{m_s}{\bar{m}_s}\left[b_s\dot{\tilde{x}}(t) + k_s\tilde{x}(t) + F_e(t)\right] + F_e(t) + b_s\dot{x}_s(t) + m_s\ddot{x}_d - \gamma sgn(S) - \lambda S - P_{est}\right\} \quad (32)$$

where $sgn(.)$ represents the signum function and γ and λ are the positive scalars, then asymptotically tracking of the system is guaranteed.

Proof: For analyzing the stability of the proposed control scheme, a Lyapunov function candidate is defined as:

$$V = \frac{S^2}{2} \tag{33}$$

The derivative of V with respect to time can be obtained as:

$$\dot{V} = S\dot{S} \tag{34}$$

By substituting (31) in (30) one can obtain:

$$\dot{V} = S\dot{S} = S[\ddot{\tilde{x}}(t) + \frac{\bar{b}_s}{\bar{m}_s}\dot{\tilde{x}}(t) + \frac{1}{\bar{m}_s}(\bar{k}_s\tilde{x}(t) + F_e(t))] \tag{35}$$

Utilizing (27) for substituting $\ddot{\tilde{x}}(t) = \ddot{x}_s - \ddot{x}_d$ in (35), yields:

$$\dot{V} = S[-\ddot{x}_d + \frac{\bar{b}_s}{\bar{m}_s}\dot{\tilde{x}}(t) + \frac{1}{\bar{m}_s}(\bar{k}_s\tilde{x}(t) + F_e(t))] + \frac{1}{m_s}[-b_s\dot{x}_s - k_s x_s + H_F(v(t)) + P_{est} - F_e - \tilde{P}(t)] \tag{36}$$

Substituting $v(t)$ from (32) in (36) yields:

$$\dot{V} = S\dot{S} = S\left[-\frac{\lambda}{m_s}S - \frac{1}{m_s}\gamma sgn(S) - \frac{\tilde{P}(t)}{m_s}\right] = -\frac{\lambda}{m_s}S^2 - \frac{1}{m_s}\gamma|S| - \frac{\tilde{P}(t)}{m_s}S \tag{37}$$

If the gain γ is selected such that condition $\gamma > |\tilde{P}(t)|$ is satisfied, (37) leads to:

$$\dot{V} \le -\frac{\lambda}{m_s}S^2 \le 0 \tag{38}$$

Equation (38) depicts that time derivative of the positive definite Lyapunov function V is negative definite. Thus, stability of the system is guaranteed. Essentially, (38) states that the squared distance to the sliding surface, as measured by S^2 decreases along all system trajectories.

Chattering phenomena is the main problem of sliding mode control and must be eliminated for the controller to perform properly. For this purpose, controller discontinuity can be smoothed out by using a saturation function $\text{sat}(S/\varphi)$ instead of sgn(S), where φ is boundary layer thickness. Therefore, control law (32) can be rewritten as follows:

$$u_s(t) = H_F^{-1}\left\{-\frac{m_s}{\bar{m}_s}[b_s\dot{\tilde{x}}(t) + k_s\tilde{x}(t) + F_e(t)] + F_e(t) + b_s\dot{x}_s(t) + m_s\ddot{x}_d - \gamma sat(S/\varphi) - \lambda S - P_{est}\right\} \tag{39}$$

To achieve a good tracking and chattering free control signal, the desired impedance and controller parameters for the piezo stage are chosen as shown in Table 1.

V. Experimental Setup

A PZT-driven nanopositioning stage with high resolution strain gage position sensor is used to perform the experiments.

Table 1
PIEZO STAGE IMPEDANCE PARAMETERS

$\bar{m}_s$	$0.8\ kg$	m_s	$2.17\ kg$
$\bar{b}_s$	$5\ ^{N.s}/_{m}$	b_s	$1078\ ^{N.s}/_{m}$
$\bar{k}_s$	$1e^5\ ^{N}/_{m}$	k_s	$3e^5\ ^{N}/_{m}$
λ	0.3	γ	250
φ	0.05		

The E500 module includes E501 piezo driver and E503 strain gage amplifier which carry out experimental data. A rigid adjustable end effector is mounted on the stage. A load cell is used to measure environmental force. A data acquisition controller (DAQ) board is used as interface element between MATLAB Real Time Workshop and the equipments. The controllers are developed in Simulink and implemented in real-time using MATLAB Real Time Workshop and through Control Desk software. A Heater is used to change the environment temperature between 25-60°C. A $T40$ sensor is also utilized for temperature monitoring (Fig. 5).

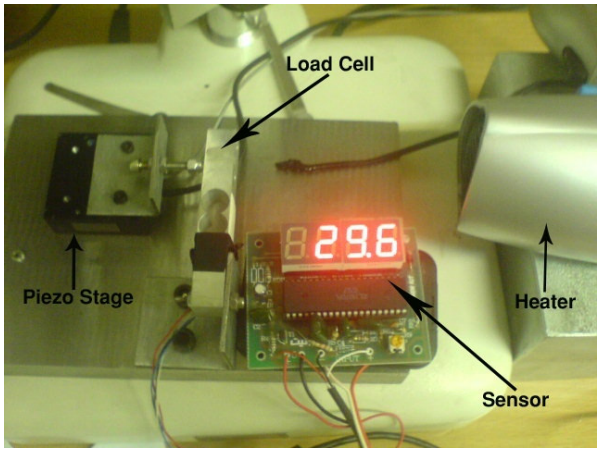

Fig. 5. The experimental setup.

VI. Experimental Results

The environmental temperature is increased from 31℃ to 45℃ and then reduced to 41℃, in a period of 75 seconds (Fig. 6). There is a space between the piezo stage and the load cell. Hence, when the alternative input signal is applied, the piezo stage contacts the load cell intermittently and generates an alternative force (Fig. 7). In Fig. 8a, the tracking of the reference signal by the proposed controller is shown for temperature of 45℃. The tracking error is plotted in the same figure, as well.

The tracking of the reference signal by the PID controller is

also investigated and the tracking error is calculated (Fig. 8b).

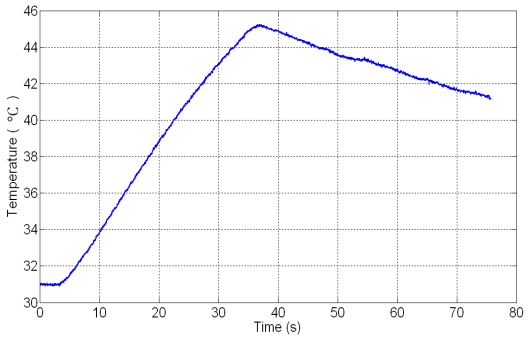

Fig. 6. The temperature variation.

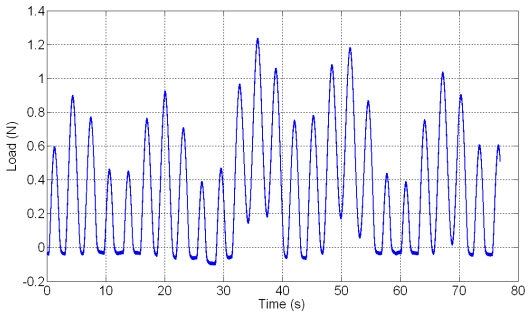

Fig. 7. The external load variation.

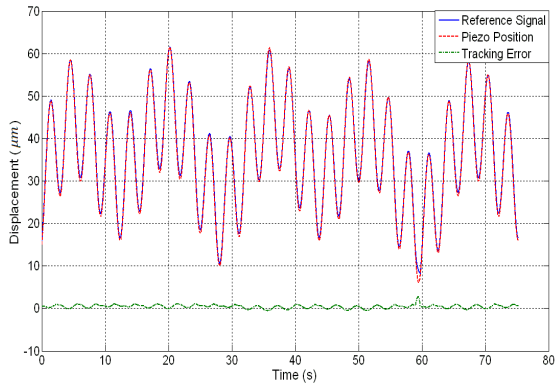

(a)

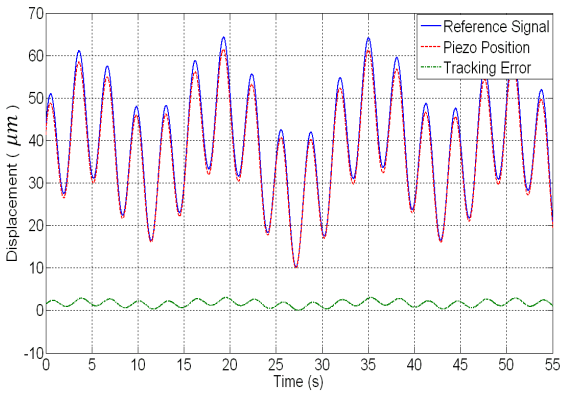

(b)

Fig. 8. (a) Tracking of the reference signal by the proposed controller. (b) Tracking of the reference signal by the PID controller.

The results show that via utilizing the proposed robust controller, the tracking error decreases noticeably.

Table 2 shows the measured performances of the PID and the proposed controllers in tracking of the desired trajectory.

VII. Conclusion

Hysteresis is the main drawback of using piezoelectric actuators in precision positioning applications. Moreover, the environmental temperature and the external load variations deteriorate the accuracy of a micromanipulation system, as well. In this paper, the Prandtl-Ishlinskii (PI) model is used to model the actuator hysteresis in feedforward scheme to cancel the hysteretic nonlinearity. A robust controller is also utilized in a feedback manner to compensate the thermal and external load disturbances effects. By implementation the proposed controller, the required transparency in micromanipulation is fulfilled.

Table 2
PERFORMANCES OF THE *PID* AND THE *PROPOSED CONTROLLERS*

Controller	$e_{max}(\mu m)$	$RMS(\mu m)$
PID	3.1	1.761
Proposed Controller	1.5	0.61

References

[1] P. Ge and M. Jouaneh, "Tracking control of a piezoceramic actuator," *IEEE Transactions on Control Systems Technology*, vol. 4, no. 3, pp. 209-215, May 1996.

[2] P. Ge and M. Jouaneh, "Generalized preisach model for hysteresis nonlinearity of piezoelectric actuators," *Precision Engineering*, 20, pp. 99-111, 1997.

[3] D. Hughes and J. T. Wen, "Preisach modeling of piezoceramic and shape memory alloy hysteresis," *Smart Mater. Struct.*, pp. 287-300, 1997.

[4] R. B. Gorbet, K. A. Morris and D. W. L. Wang, "Passivity-based stability and control of hysteresis in smart actuators," *IEEE Transactions on Control Systems Technology*, vol. 9, January 2001.

[5] P. Ge and M. Jouaneh, "Modeling hysteresis in piezoceramic actuators," *Precision Engineering*, 17 (3), 211-21, 1995.

[6] K. Kuhnen and H. Janocha, "Inverse feedforward controller for complex hysteretic nonlinearities in smart-material systems," *Control and Intelligent Systems Journal*, 2001.

[7] K. Kuhnen and H. Janocha, "Adaptive inverse control of piezoelectric actuators with hysteresis operators." *Proceedings of European Control Conference (ECC), Karsruhe,* August 1999.

[8] S. Bashash and N. Jalili, " Robust multiple frequency trajectory tracking control of piezoelectrically driven micro/nanopositioning systems," *IEEE Transactions on Control Systems Technology*, vol. 15, no. 5, pp. 867-878, 2007.

[9] H. Elmali and N. Olgac, "Sliding mode control with perturbation estimation (SMCPE): A new approach," *Int. J. Control*, vol. 56, pp. 923–941, 1992.

[10] H. Elmali and N. Olgac, "Implementation of sliding mode control with perturbation estimation (SMCPE)," *IEEE Trans. Control Syst. Technol.*, vol. 4, no. 1, pp. 79–85, 1996.